I&EC research
Industrial & Engineering Chemistry Research

Article

pubs.acs.org/IECR

Acidic and Catalytic Properties of Modified Clay for Removing Trace Olefin from Aromatics and Its Industrial Test

Xin Pu, Nai-wang Liu, Zheng-hong Jiang, and Li Shi*

The State Key Laboratory of Chemical Engineering, East China University of Science and Technology, Shanghai 200237, People's republic of China

ABSTRACT: The commercial clay modified with zeolite and La_2O_3 was characterized by thermoprogrammed desorption (t.p.d.) of NH_3 and pyridine adsorption followed by Fourier transform infrared spectroscopy (FTIR). The result showed that the weak Lewis acid plays an important role in the alkylation reaction between olefin and aromatics which obeyed the carbonium ion mechanism. The industrial test was conducted in the 450kt/a industrial PX device at Sinopec Zhenhai Company for removing trace olefins from aromatics. It has been proved that the life cycle of the catalyst was 5.3 times that of the commercial clay. The kinetics formula for deactivation rates was explored and the result showed that the rate of clay was much higher than the catalyst deactivation rate.

1. INTRODUCTION

Aromatic hydrocarbon, an important raw material in petrochemical processes and refineries, can be obtained from the reforming and cracking process. However, these aromatic streams always contain undesirable trace olefins[1] which are harmful to the following technological processes and the applications of aromatics.[2] Commercial clay was widely used to remove these olefins in most refineries with the drawbacks of limited lifetime and pollution.

Clays are very versatile materials and hundreds of millions of tons find applications not only in ceramics and building materials, paper coatings and fillings, drilling muds, foundry molds, pharmaceuticals, etc., but also as adsorbents,[3,4] catalysts[5] or catalyst supports,[6] ion exchangers, chattonella marina,[7] etc., depending on their specific properties.[8] Because of its physical and chemical properties (i.e., large specific surface and adsorptive affinity for organic and inorganic ions), clay has attracted more and more attention as a new type of microporous solid that can serve as a separating agent or sorbent, etc.[9] In particular, the clay modified by metal halides is noteworthy for removal of trace olefins from aromatics.[10] It is also promising from the ecological point of view because the modified clay, which had much better catalytic activity, considerably reduces the consumption of the commercial clay and the emission of solid waste at refineries.

Indeed, we have synthesized the novel solid acid catalyst based on modified clay. It was found that the synthesized catalyst could prolong the effective running time and the material present the Brønsted and Lewis acidity, especially the weak Lewis acid, which was the main reason for the enhancement of the effective reaction time.[11]

Obviously, the acidity plays a role in this particular behavior. In this work, the acidity of the catalyst was characterized by thermoprogrammed desorption (t.p.d.) of NH_3 and pyridine adsorption followed by Fourier FTIR. The object is to estimate quantitatively the number of acid sites, the acid strength, and the distribution of acid sites.

The industrial test were carried on the 450Kt PX combination units which consist of xylene rectification, xylene isomerization, alkylation and transalkylation, toluene disproportionation, and PX adsorption in ZRCC (Sinopec Zhenhai Refining and Chemical Co.). The adsorbent in PX adsorption part requires the bromine index (BI) of the feedstock to be lower than 20 mgBr/100 g. To protect the adsorbent, clay towers were used to remove the olefinic compounds before the aromatic was introduced into the adsorption tower. In this work, the clay tower was filled with the synthesized catalyst.

2. EXPERIMENTAL SECTION

2.1. Materials. The acid activated bentonitic clay used as support in this study was produced in Zhejiang province, China. The components of the clay are shown in Table1. The texture properties of clay can be found in Table 2.

Table 1. Components of Active Clay

component	content *W*, %
SiO_2	60.3
Al_2O_3	15.3
Fe_2O_3	7.8
CaO	2.1
MgO	7.3
K_2O	1.6
Na_2O	0.9
other	4.7

Table 2. Textural Properties of Clay

	surface area (m^2/g)	micropore area (m^2/g)	pore volume (cm^3/g)	pore diameter (nm)
clay	195.78	24.16	0.1864	5.769

Received: June 27, 2012
Revised: October 5, 2012
Accepted: October 8, 2012
Published: October 8, 2012

dx.doi.org/10.1021/ie301706s | *Ind. Eng. Chem. Res.* 2012, 51, 13891−13896

The zeolite used in our experiment was MCM-22 purchased from Nanjing, China.

The BI of the aromatic hydrocarbons was about 950−1500 mgBr/100 g and the components are shown in Table 3.

Table 3. Components of the Aromatic Hydrocarbon

component	content *W*, %
nonaromatic	<1
toluene	<0.5
ethylbenzene	10
p-xylene	10
m-xylene	23
o-xylene	12
C9 aromatic	30
C9+ aromatic	14
C=C	950−1500 mgBr/100 g

2.2. Catalyst Preparation. As shown in Figure 1, the procedures of catalyst preparation were as follows. First, the

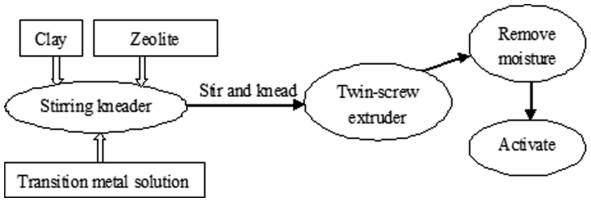

Figure 1. The procedure of industrial production.

acid activated bentonitic clay and the MCM-22 zeolite (the proportion of the clay and the MCM-22 is 4) were mixed completely in a mixing kneader. Then La_2O_3 (7 wt %) and a suitable amount of nitric acid were added. Second, the raw materials which had been mixed through stirring for 0.5 h were sent to the twin-screw extruder by the conveying systems. Third, the moisture of the extrudate was removed in an oven at 393 K in a 2-h drying process; and finally the extrudate was baked at 823 K for 6 h.

2.3. Catalytic Tests in the Laboratory. The catalytic activity tests were carried out in a fixed-bed tubular microreactor, equipped with a constant-flow pump to control flow rate and a controlled heating system to maintain the required temperature. Two milliliters of the catalyst was loaded in the middle of the reactor, with the spare spaces were filled with quartz sand (40−60 mesh). The experiments were carried out at a reaction temperature of 448 K, a reaction pressure of 1 MPa, and a WHSV of 30 h^{-1}. The inlet and effluent liquid from the reactor were analyzed by a bromine index analyzer. The olefins conversion rate was as follows: $(X) = [(n_o - n_i)/n_o] \times 100$, where n_o was the initial content of olefins and n_i was the final content of olefins.

2.4. Catalyst Characterization. Temperature-programmed desorption experiments were done in a Micromeritics 2920 apparatus. The as-synthesized catalyst (100 mg) was preactivated in the helium streem over 2 h at 523 K, and then NH_3 was adsorbed at 318 K. Desorption was carried out at a heating rate of 10 deg min^{-1}.

FTIR measurements were carried out with pyridine as the probe molecule. The Fourier transform infrared spectra were collected (Magna-IR 550, Nicolet Company) with a combined reactor-spectrometer system, using a low-volume in situ cell with a water-cooled KBr window (see Figure 2). For all experiments, 16.5−16.9 mg of finely ground catalyst or

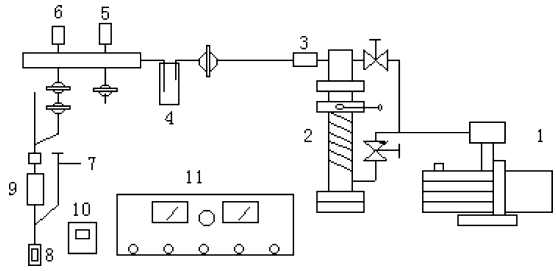

Figure 2. In situ FTIR reactor system: (1) rotary vane vacuum pumps; (2) high-vacuum oil diffuse pump; (3) antihunting device; (4) buffer unit; (5) vacuum gauge; (6) thermocouple well; (7) pyridine entrance; (8) infrared transmission windows; (9) heater coil; (10) temperature controller and solid state relays; and (11) composite vacuum table.

commercial clay was pressed into self-supporting wafers with a diameter of 10 mm. The wafer loaded into the cell was pretreated at 653 K under vacuum conditions for 2 h and cooled to 353 K for pyridine adsorption. The physisorbed pyridine was eliminated at 473 K. The total concentrations of Brønsted and Lewis sites able to retain pyridine at 473 K were determined by using the absorbance surfaces of the corresponding bands at 1540 and 1450 cm^{-1}, respectively.[12,13]

Then the sample was subjected to thermal desorption at 723 K followed by the IR measurement. Through the FTIR spectroscopy, the strong acid sites can be monitored. The weak acid sites can be calculated.

2.5. Industrial Test. Figure 3 shows the flow chart of the industrial application test in ZRCC. The aromatics flow

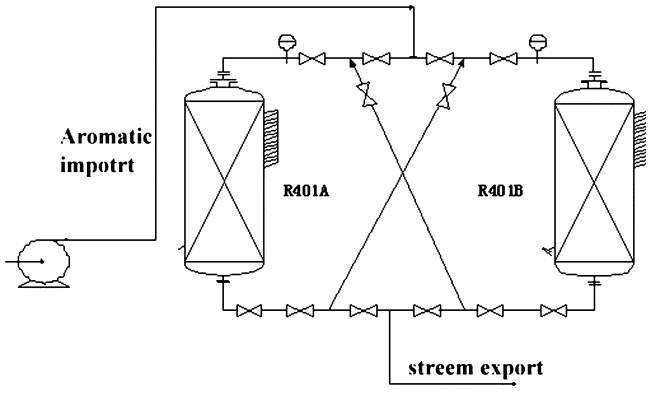

Figure 3. Flow chart of the industrial application test process.

through tower R401A loaded with commercial clay, then flow through tower R401B, which was filled with 100 tons of catalysts.

The reactor is constructed as a fixed bed reactor from stainless steel. Its design pressure is 2.5 MPa and the design temperature is 600 K with an inner diameter of 3.4 m and a height of 17.2 m. For equal distribution of the feed, the reactor is equipped with a redistributer, Φ20 ceramic balls. The 100 tons of catalysts were loaded in the center of the fixed-bed reactor, between two ceramic balls. At the bottom of the reactor, there are several layers of inert ceramic balls and a stainless steel sieve is installed to hold the catalyst.

dx.doi.org/10.1021/ie301706s | *Ind. Eng. Chem. Res.* 2012, 51, 13891−13896

The reactor operating temperature was about 443 to 453 K, controlled by regulating the steam flow. The reaction pressure was 1.0 MPa and the volume space velocity was about1.2 h^{-1}.

3. RESULTS AND DISCUSSION

3.1. Catalytic Acitivity in the Laboratory. The activity of different samples was investigated in the laboratory, and the results are presented in Figure 4. It was demonstrated that the

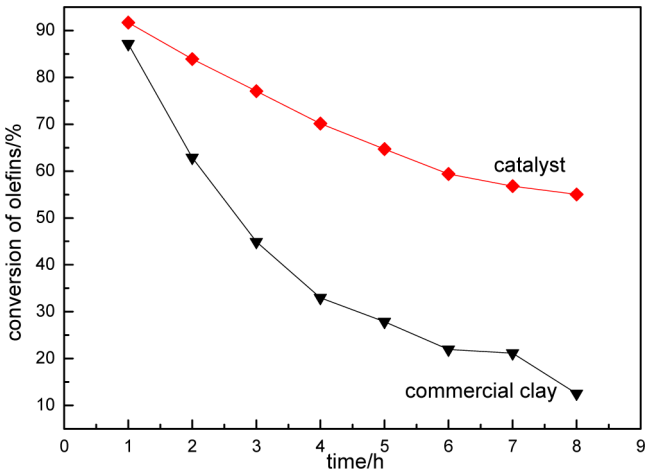

Figure 4. Conversion of olefins of different samples in the laboratory.

synthesized catalyst showed great superiority to the commercial clay. At the end of the 8-h reaction, the catalyst maintained an olefins conversion of more than 55% over the reaction duration, while that of the commercial clay was 2.5 h. It can be concluded that the synthesized catalyst can prolong the lifetime more than the commercial clay.

3.2. Characterization of the Acidity by Pridine Adsorption. The acidity of the catalyst and commercial clay measured by t.p.d. in cm^3 of adsorption of NH_3/g is presented in Figure 5. The original t.p.d. graphs of samples show two

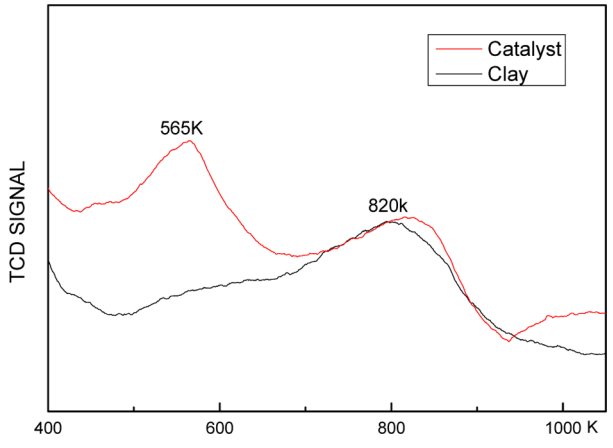

Figure 5. Thermoprogrammed desorption/NH_3 graphs.

distinct peaks at 565 and 820 K assigned to weak acid sites and strong acid sites, respectively. The weak acid of catalyst was much higher than that of clay.

The t.p.d. method itself does not allow one to assign the peaks. On the basis of the IR result (Figure 6) we suggest that both Lewis and Brønsted centers contribute to each peak, but the latter sites participate in the overall pattern to a lesser extent.

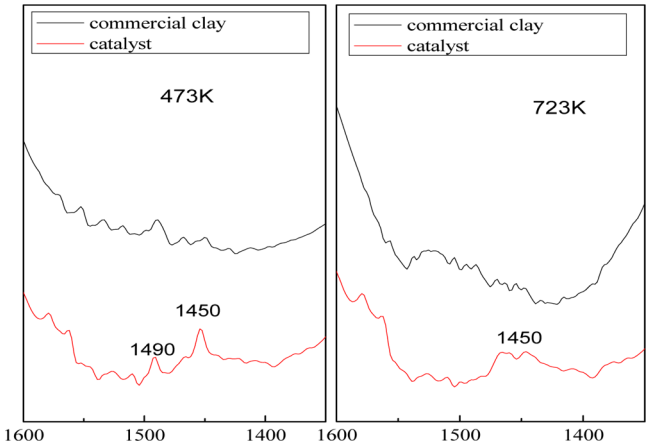

Figure 6. FTIR spectra of pyridine adsorbed on different samples at 473 and 723 K.

Acidity distribution has been monitored by using pyridine adsorption/desorption (Figure 6 and Table 4). The spectrum

Table 4. Acidic Properties of Different Samples

	acidity (× 10^{-4} mol·g^{-1})		
sample	total L acid sites	strong L acid sites	weak L acid sites
catalyst	3.17	0.24	2.93
clay	0.32	0.14	0.18
MCM-22	25.39	18.69	6.70

displayed many bands in the wavenumber range of 1400−1600 cm^{-1}, which was attributed to the interaction of pyridine with Lewis (L) and Brønsted (B) acid sites on the sample surfaces. The spectra present bands of adsorption at 1450 and 1490 cm^{-1}, which is typical of adsorbed pyridine. The fingerprint pyridine bands corresponding to Lewis sites appear at 1450 cm^{-1}, which is typical of adsorbed pyridine (PyrL).[14,15] It mainly observed the band at around 1450 cm^{-1}, arising due to 19b ν(C−C) vibration of pyridine adsorbed at Lewis acid sites. Another band could be seen at around 1490 cm^{-1} due to contributions of both the Lewis and Brønsted acid sites.[16] There is no band observed at 1540 cm^{-1}, so the amount of Brønsted acid could not be calculated. Table 4 shows the amount of the total L acid, weak L acid, and strong L acid which were calculated by the Lambert−Beer law. The acid site concentration was the following: $C_L = (3.73 \times 10^{-4})A_L$, where C_L was the amount of the L acid sites, and A_L was the peak area at 1450 cm^{-1} in Figure 6. The amount of total L acid can be calculated from the IR spectrum at 473 K, while that of strong L acid sites can be obtained from the IR spectrum at 723 K.

According to Table 4, it is obvious that the catalyst was higher than commercial clay in the amount of weak L acid, with 2.93×10^{-4} mol·g^{-1} weak L acid. This was in accordance with the catalytic activity data, and it can be concluded that the increase in activity of the catalyst contributed to the increase in the amount of weak L acid.

The total amount of L acid in the zeolite was 25.39×10^{-4} mol·g^{-1}, and the amount of weak L acid was 6.70×10^{-4} mol·g^{-1}. It should be noted that the amount of strong L acid was 18.69×10^{-4} mol·g^{-1}. When the clay mixed with the

dx.doi.org/10.1021/ie301706s | Ind. Eng. Chem. Res. 2012, 51, 13891−13896

zeolite, the amount of L acid in the catalyst became higher than that of the clay. The zeolite can adjust the amount of acid in the catalyst. The zeolite has a large amount of strong L acid which can cause the olefins to polymerize with each other.[17] This was the reason why we only add 20% zeolite in catalyst.

The amount of the weak L acid in the commercial clay was only 0.18×10^{-4} mol·g^{-1} and this explained why the commercial clay activity was much poorer than the catalyst in Figure 4.

It was well-known that the alkylation of aromatic with olefins over solid acid catalyst obeyed the generally accepted carbonium ion mechanism.[18] The olefin molecule was protonated by the L acid sites to a carbonium ion that generated, by electrophilic attack on the aromatic π-electrons, a mono- or polyalkylbenzenium ion. The desorption process and the loss of the proton gave the alkylated aromatic and restored the L acid sites. The process is illustrated in Scheme 1.

Scheme 1. The Reaction between Olefin and Aromatics

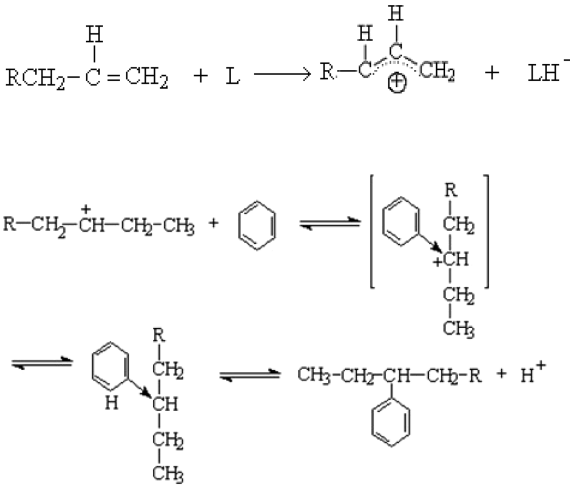

3.3. Industrial Test Results. One hundred tons of catalysts loaded in tower R401B were used in the industrial application test in the Sinopec Zhenhai Refining and Chemical Company. The samples collected from the bottom of the reactor were measured for the bromine index every day.

Figure 7 shows the changing of the bromine index of aromatics after reaction over the catalyst at industrial test with increasing time. For comparison, the data of the commercial clay also can be found from Figure 7. The bromine index of aromatics with the catalyst remained less than 20 for 16 days. As for the commercial clay, the effective reaction time only lasts about 3 days. It should be noted that it took 8 days for the bromine index to change from 20 to 50 while the commercial clay took only 4 days for the same change.

It is obvious that the commercial clay (treated as a type of catalyst) has a higher catalyst deactivation rate in comparison with our novel catalyst. By using the power law equation for catalyst and clay, it is possible to write formulas for deactivation rates of catalyst. As shown in Figure 8:

$$X_o = 56.36(27.4 - t)^{0.173} \quad \text{for synthesized catalyst} \qquad (1)$$

$$X_o = 55.81(7.8 - t)^{0.241} \quad \text{for commercial clay} \qquad (2)$$

where t is time and X_o is olefin conversion. Assuming that the deactivation rate of catalyst and clay can be written as a general

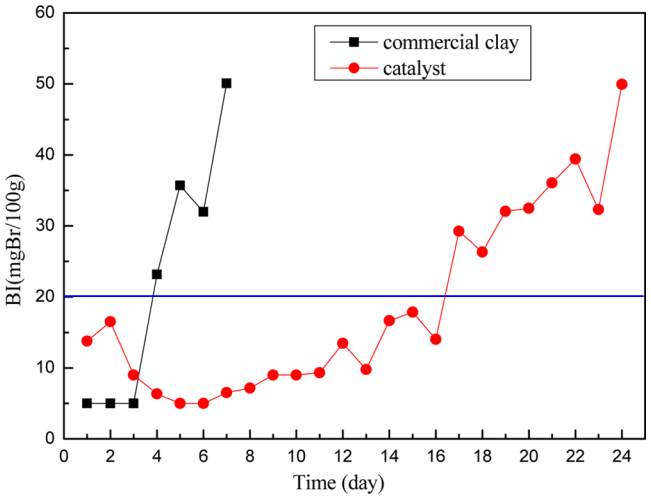

Figure 7. The bromine index of aromatics after reaction.

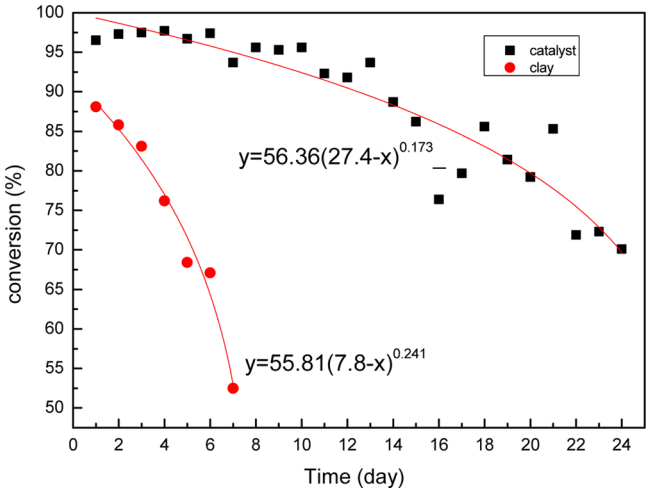

Figure 8. Conversion of olefins in the industrial application test.

form in order to derive the kinetics formula for deactivation rates:[19,20]

$$-dX_o/dt = KX_o^n \qquad (3)$$

where n is the degree of reaction and K is an integral parameter and must be determined for both equations. After integration and calculation, degrees of reaction and integral parameters were determined as follows:[21]

$$-dX_o/dt = (2.28 \times 10^9)X^{-4.78} \quad \text{for synthesized catalyst} \qquad (4)$$

$$-dX_o/dt = (4.12 \times 10^6)X^{-3.14} \quad \text{for commercial clay} \qquad (5)$$

These formulas indicated that the deactivation rate of clay was much higher than that of the synthesized catalyst.

The commercial clay has a large surface area and relatively high pore volume, while once the commercial clay reaches adsorption equilibrium, it will be deactivated soon.

3.4. Comparison of the Refined Product. The gas chromatography-flame ionization detection (GC-FID) analyses were carried out on a Hewlett-Packard Model HP5890 gas chromatograph equipped with a capillary column (AT-WAX, 50 m length, 0.32 mm inner diameter, 0.30 μm film thickness)

dx.doi.org/10.1021/ie301706s | Ind. Eng. Chem. Res. 2012, 51, 13891−13896

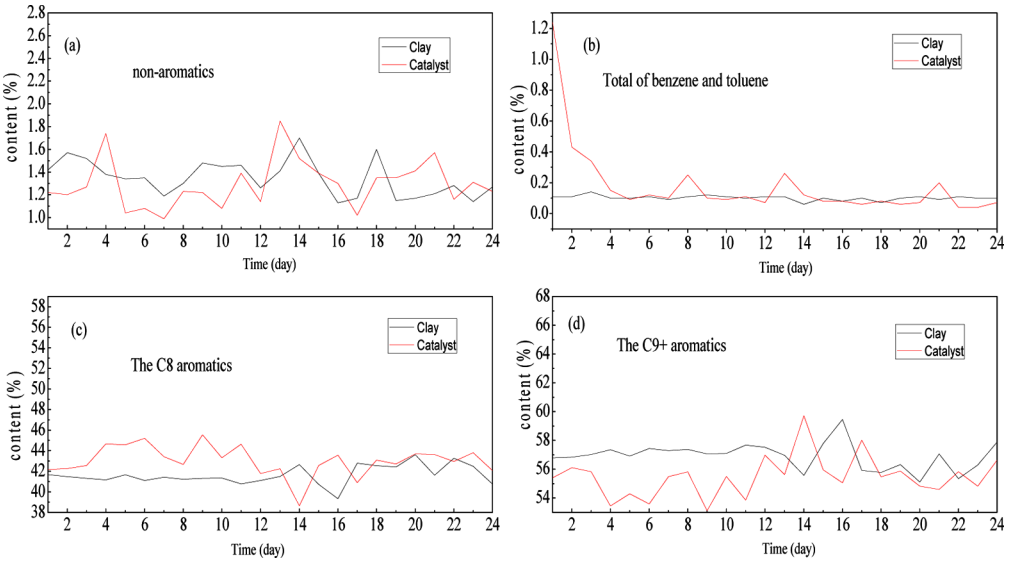

Figure 9. Comparison of the refined product of synthesized catalyst and clay.

for investigating the changes in the content of aromatics after reaction.

The catalyst filled in tower R401B and the commercial clay filled in tower R401A were compared on their performance (Figure 9).

The refining product treated by the synthesized catalyst has higher content of C8 (ethylbenzene, *p*-xylene, *m*-xylene, and *o*-xylene) than did the commercial clay (Figure 9c), but with lower content of C9+ aromatics (Figure 9d). This may be attributed to that more acid sites in the synthesized catalyst with a large number of acid sites could catalyze the olefins to alkylate with aromatic hydrocarbon or polymerize each other.[17] From Figure 9a, the content of nonaromatics did not have distinct changes after treatment by synthesized catalyst. It should be noted that the concentration amount of benzene and toluene was higher after catalyst treatment than that of refining product of commercial clay at the preliminary stage of the reaction (Figure 9b), which demonstrated that the process of removal of trace olefins by the synthesized catalyst undergoes some chemical reactions. It was worthy of note that this phenomenon only lasts 3 days.

The comparison implied that the distribution of the aromatics after being hydrotreated by the synthesized catalyst tended to increase the amount of xylene, which was in accord with the aim of the PX combination units.

4. CONCLUSIONS

In agreement with Onida et al.,[22] the Lewis and Brønsted acid sites both contribute to the absorption bands of pyridine, but the latter sites participate in the overall patern to a lesser extent from the acid characterization in this work. It can be concluded that the weak L acid site was the main reason for enhancement of the effective reaction time.

The catalyst shows a great superiority over the commercial clay. The industrial application test presented that the effective reaction time of the catalyst lasts 16 days, about 5.3 times as long as that of the commercial clay. By reducing the frequency of clay replacement and landfill quantity, this catalyst will significantly reduce production cost and protect the environment. The study on kinetics formula indicated that the deactivation rate of clay was much higher than that of the synthesized catalyst.

The analysis of the refined product showed that our synthesized catalyst did not have any disadvantage for the quantity or distribution of the aromatic hydrocarbons. What was better was the xylene, the desired product of the PX combination units, had a higher concentration after the treating.

AUTHOR INFORMATION

Corresponding Author

*E-mail: yyshi@ecust.edu.cn. Phone: 021-64252274.

Notes

The authors declare no competing financial interest.

ACKNOWLEDGMENTS

The authors would like to express their thanks to the Sinopec Zhenhai Refining and Chemical Company for their help during the industrial application test.

REFERENCES

(1) Brown, S. H.; Waldecker, J. R.; Lourvanij, M. Process for reducing Bromine Index of hydrocarbon feedstocks. U.S. Patent 744750, 2005.

(2) Chen, C. W.; Wu, W. J.; Zeng, X. S.; Jiang, Z. H.; Shi, L. Study on several mesoporous materials catalysts applied to the removal of trace olefins from aromatic and commercial sidestream tests. *Ind. Eng. Chem. Res.* **2009**, *48*, 10359−10363.

(3) Renedo, M. J.; Fernando, G.; Carmen, P.; Josefa, F. Study of Sorbents Prepared from Clays and CaO or $Ca(OH)_2$ for SO_2 Removal at Low Temperature. *Ind. Eng. Chem. Res.* **2006**, *45*, 3752−3757.

(4) Aysegul, E. M. Removal of sulphur Dioxide from Flue Gases. *Energy Sources, Part A* **1999**, *21*, 611−619.

(5) Mikhail, S.; Zaki, T.; Khalil, L. Desulfurization by an Economically Adsorption Technique. *Appl. Catal., A* **2002**, *227*, 265−278.

(6) Dhakshinamoorthy, A.; Pitchumani, K. Clay-supported Ceric Ammonium Nitrate as an Effective, Viable Catalyst in the Oxidation of Olefins, Chalcones and Sulfides by Molecular Oxygen. *Catal. Commun.* **2009**, *10*, 872−878.

(7) Wu, T.; Yan, X. Y.; Cai, X.; Tan, S. Z.; Li, H. Y.; Liu, J. S.; Yang, W. D. Removal of Chattonella marina with clay minerals modified with a Gemini surfactant. *Appl. Clay Sci.* **2010**, *50*, 604−607.

(8) Vaccari, A. Clays and Catalysis: a Promising Future. *Appl. Clay Sci.* **1999**, *14*, 161−198.
(9) Hana, Y. S.; Yamanakab, S. J.; Choya, J. H. A New Thermally Stable $SiO_2 \pm Cr_2O_3$ Sol Pillared Montmorillonite with High Surface Area. *Appl. Catal., A* **1998**, *174*, 83−90.
(10) Li, G. L.; Luan, J. N.; Zeng, X. S.; Shi, L. Removal of Trace Olefins from Aromatics over Metal-Halides-Modified Clay and Its Industrial Test. *Ind. Eng. Chem. Res.* **2011**, *50*, 6646−6649.
(11) Luan, J. N.; Li, G. L.; Shi, L. Study of Modified Clay and Its Industrial Testing in Aromatic Refining Ind. *Eng. Chem. Res.* **2011**, *50*, 7150−7154.
(12) Guisnet, M.; Ayrault, P.; Datka, J. Acid Properties of Dealuminated Mordenites Studied by IR Spectroscopy. 2. Concentration, Acid Strength and Heterogeneity of OH Groups. *Pol. J. Chem.* **1997**, *71*, 1455−1461.
(13) Guisnet, M.; Ayrault, P.; Countanceau, C.; Alvarez, M. F.; Datka, J. Acid properties of dealuminated beta zeolites studied by IR spectroscopy. *J. Chem. Soc., Faraday Trans.* **1997**, *93*, 1661.
(14) Hoang, V. T.; Qing, Ll. H.; Adrian, U.; Mladen, E.; Do, T. On.; Serge, K. Effect of the acid properties on the diffusion of C7 hydrocarbons in UL-ZSM-5 materials. *Microporous Mesoporous Mater.* **2006**, *92*, 117−128.
(15) Awate, S. V.; Waghmode, S. B.; Agashe, M. S. Synthesis, characterization and catalytic evaluation of zirconia-pillared montmorillonite for linear alkylation of benzene. *Catal. Commun.* **2004**, *5*, 407−411.
(16) Kalita, P.; Gupta, N. M.; Kumar, R. Synergistic role of acid sites in the Ce-enhanced activity of mesoporous Ce-Al-MCM-41 catalysts in alkylation reactions: FTIR and TPD-ammonia studies. *J. Catal.* **2007**, *245*, 338−347.
(17) Lenarda, M.; Storaro, L.; Ganzerla, R. Hydroformylation of simple olefins catalyzed by metals and clusters supported on unfunctionalized inorganic carriers. *J. Mol. Catal. A: Chem.* **1996**, *111*, 203−237.
(18) Lenarda, M.; Storaro, L.; Pellegrini, G.; Piovesan, L.; Ganzerla, R. Solid acid catalysts from clays Part 3: benzene alkylation with ethylene catalyzed by aluminum and aluminum gallium pillared clays. *J. Mol. Catal. A: Chem.* **1999**, *145*, 237−244.
(19) Pour, A. N.; Shahri, S. M. K.; Zamani, Y.; Irani, M.; Tehrani, S. Deactivation studies of bifunctional Fe-HZSM5 catalyst in Fischer−Tropsch process. *J Nat. Gas Chem.* **2008**, *17*, 242−248.
(20) Zhou, W.; Chen, J. G.; Fang, K. G.; Sun, Y. H. The deactivation of Co/SiO_2 catalyst for Fischer−Tropsch synthesis at different ratios of H_2 to CO. *Fuel Process. Technol.* **2006**, *87*, 609−616.
(21) Pour, A. N.; Housaindokht, M. R.; Tayyari, S. F.; Zarkesh, J. Deactivation Studies of Nano-structured iron Catalyst in Fischer−Tropsch Synthesis. *J Nat. Gas Chem.* **2010**, *19*, 333−340.
(22) Onida, B.; Geobaldo, F.; Testa, F.; Crea, F.; Garrone, E. FTIR investigation of the interaction at 77 K of diatomic molecular probes on MCM-22 zeolite. *Microporous Mesoporous Mater.* **1999**, *30*, 119−127.